Nigerian Journal of Applied Physics (NJAP)
ISSN Print: ISSN: 3115-5871
ISSN Online : 3115-588X
DOI: https://doi.org/10.62292/njap-v1i1-2025-22
Volume 1(1), September 2025

Optimisation of Polyacrylic Acid Usage as Surfactant in Hydrothermally Synthesised Cu_2ZnSnS_4 Thin Films for Application as Counter Electrode in Dye Sensitised Solar Cell

***[1]Kasim Ibrahim Mohammed, [2]Kasim Uthman Isah, [2]Uno Essang Uno, [2]Abdullahi Mann, [1]Mohammed Ahmed, [1]Najeebullah Yahuza and [3]Nafarizal Nayan**

[1]Department of Physical Sciences, Niger State Polytechnic Zungeru
[2]Department of Physics, Federal University of Technology Minna
[3]Microelectronics and Nanotechnology Shamsuddin Research Centre (MiNT-SRC), Institute for Integrated Engineering (I^2E), Universiti Tun Hussein Onn Malaysia

*Corresponding author's email: kasimzabbo@yahoo.com Phone: +2348059067132

ABSTRACT
Cu_2ZnSnS_4 (CZTS) being an earth abundant material are non-toxic, low cost and belongs to the third generation photovoltaic (PV) material when used as counter electrode in dye sensitised solar cells. CZTS nanoparticle slurries were synthesised using hydrothermal method for application as counter electrode in dye sensitised solar cells. In order to optimise the synthesis process, the polyacrylic acid (PAA) used as surfactant in the precursor solution was varied thus: 0.0 g, 0.6 g, 1.0 g and 1.4 g. The XRD revealed peaks of CZTS (112) and (220) for the sample synthesised using 1.0 g PAA and in addition, numerous other peaks were observed for the remaining samples. The crystallite sizes ranged between 7 and 19 nm. Raman spectra of the films reveal CZTS peaks of 338, 351 and 252 cm^{-1} for samples synthesised using 1.0 g PAA precursor while ZnS, SnS, Cu_3SnS_3, Cu_3SnS_4, Sn_2S_3 secondary and ternary phases were observed for other amounts in addition to the 338 CZTS peak. SEM image show spherical nanoparticles and agglomerated nanosphere-like shapes. The Cu: Zn: Sn: S atom ratios were close to stoichiometry for 1.0 g polyacrylic acid and 0.6 g PAA. The surface roughness was between 800 and 1500 nm. The bandgap ranged between 1.51 eV and 1.54 eV. In order to test for the photovoltaic activity of the best CZTS materials film sample, it was used as a counter electrode in dye sensitised solar cell. The assembled cell after characterisation yielded an energy conversion efficiency of 3.2%.

Keywords:
CZTS,
Hydrothermal,
Surfactant,
Polyacrylic acid.

INTRODUCTION

Cu_2ZnSnS_4 (CZTS) has been intensively examined as an alternative PV material due to its similarity in material properties with $CuInGaSe_2$ (CIGS) and the relative abundance of raw materials (Washio *et al*., 2015). CZTS thin films being an earth abundant material are non-toxic, low cost and belong to the second generation PV material in thin film solar cells and third generation PV material when used as counter electrode in dye sensitised solar cells, in which the active bulk-material, used as absorber layer and counter electrode in the standard PV technology is replaced by a thin film, with typical thickness of micron. The huge reduction of the active material requirement in respect to the standard technology allows a large decrease of the device costs (Chopra *et al*., 2024). CZTS have high absorption coefficient which is (> 10^4 cm^{-1}) and a desirable direct band gap (~1.45 eV), as a result, its thin film has been considered an excellent PV material. Theoretical calculations have shown that conversion efficiency as high as 32% is possible for CZTS TFSCs with a CZTS layer of several micrometers (Ito and Nakazawa, 1988). Wadia *et al*. (2009) also calculated the minimum raw materials cost for the existing PV technology and the emerging PV technology and concluded that the cost of raw material for CZTS PV technology is much lower than that of the existing PV technologies.

Dye-sensitized solar cells (DSSCs) are unique when compared to other solar cells because the electron transport, hole transport and light absorption are all handled by different materials in the cell. The dye acts as

the absorber material and is anchored to a wide band gap semiconductor (usually metal oxides) such as titanium oxide, tin oxide or zinc oxide. When the dye absorbs light energy, the excited electron rapidly drifts from the valence to the conduction band of the semiconductor material, which carries the electron to the photoelectrodes. A redox couple (using an electrolyte) then reduces the oxidized dye back to its neutral state and transports the positive charge to the counter-electrode. The most employed dye in DSSCs is the ruthenium based dye and an iodide/triiodide redox couple as electrolyte. Recent research into organic dyes with a lower band gap using a cobalt reduction couple has led to power conversion efficiency (PCE) of 12.3% (Hardin *et al*., 2012). The counter electrode (CE) being a critical component of DSSCs plays an important role in catalysing the reduction of I_3^- to I^- to regenerate the sensitiser. Generally, CE with both superior catalytic activity and good conductivity is indispensable for getting better PCE (Yang *et al*., 2016). Platinum (Pt) has been widely used as CE material for DSSCs owing to its excellent catalytic activity and conductivity characteristics (Yan *et al*., 2016). However, due to scarcity and high cost of Pt, it is limited in its use. Recently, extensive effort has been made to develop low-cost and high-efficiency platinum-free CE materials. Among them, transition metal sulphides have been explored as CE owing to both their excellent electro-catalytic activity and conductivity (Chang *et al*., 2023). Some of these transition metal sulphides are Cu_2ZnSnS_4 (CZTS), $Cu_2ZnSn(S,Se)_4$ (CZTSSe) and $Cu_2ZnSnSe_4$ which are a class of earth-abundant and environmental friendly materials and has been regarded as one of the most promising photovoltaic materials in solar-energy conversion and energy storage. One key attention is derived from positive synergetic effect within the different components in CZTS, which is more conducive to improve the catalytic activity in solar cell. CZTS material could also significantly cut down the cost of the cell. In the recent years, there have been lots of reports about CZTS as CEs for solar cell. CZTS could be prepared with different structure and morphology (nanocrystals, two-dimensional plate arrays, hierarchical nanostructures, nanofibers, and nanospheres) using different methods (hot-injection, solvothermal process, spray deposition, electrospun, and precursor process), which affected the catalytic performance for reduction of I_3^- (Wei *et al*., 2016).

In 1991, Gratzel and co-workers reported the first DSSC, which attracted attention immediately because of high-efficiency (~12%) on small areas, potential low cost, environmental friendliness and simple-fabrication procedure. DSSCs have become one of the most promising photovoltaics as an alternative to the conventional silicon semiconductor solar cells. A DSSC is mainly composed of dye sensitised semiconductor electrode (working electrode), redox active electrolyte, and the CE. A typical DSSC is usually assembled in a sandwich type device with dye anchored nano-crystalline TiO_2 films as photo-anode, platinised conductive glass as CE, and I_3^-/I^- in organic solvent as electrolyte solution (Zhengfu *et al*., 2014). The principle of operation of the DSSCs is shown in Figure 1 with different pathways of electron movement. Upon illumination of DSSCs, the dye molecule becomes photo-excited and ultrafast electrons are injected into the conduction band of the semiconductor electrode. Then the original state of the dye is subsequently restored by electron donation from the electrolyte which is usually a solution of an organic solvent or ionic liquid solvent containing the I_3^-/I^- redox system (Anurag *et al*., 2018).

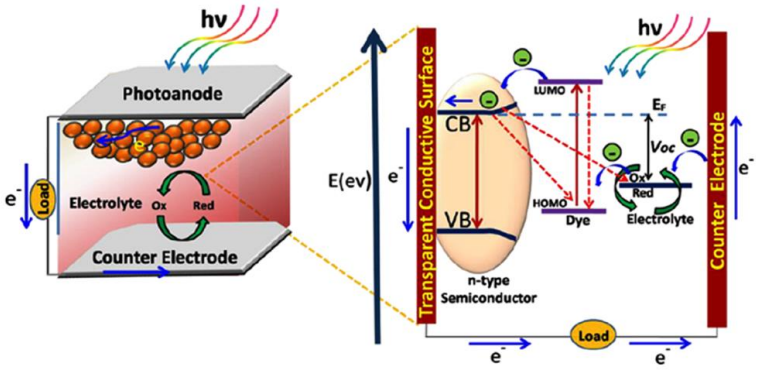

Figure 1: General architecture and principle of operation of dye sensitised solar cells (Malerba, 2014)

The CE is a critical component of DSSCs that plays an important key role in catalysing the reduction of triiodide to iodide (I_3 - to I-) to regenerate the sensitizer. Generally, CE with both superior catalytic activity and good conductivity is indispensable for getting better power conversion efficiency (PCE). Platinum (Pt) has been widely used as CE material for DSSCs owing to above-mentioned characteristics. However, the use of platinum

(Pt) is limited by its relatively scarce and resulting expensive price. Recently, extensive effort has been made to develop low-cost and high-efficiency platinum-free CE materials. Among them, transition metal sulphides have been explored as CE owing to both their excellent electro catalytic activity (Shuang *et al*., 2018).

$Cu_2ZnSnSe_4$ are a class of earth-abundant and environmental friendly materials, which has been regarded as one of the most promising photovoltaic materials in solar-energy conversion and energy storage. One key advantage is the positive synergetic effect of different components in CZTS, which is more conductive to improve the catalytic activity in solar cell. Besides, it could significantly cut down the cost of cell. In the recent years, there have been lots of reports about CZTS as CEs for solar cell. CZTS material can be prepared with different structure and morphology (nanocrystals, two-dimensional plate arrays, hierarchical nanostructures, nanofibers, and nanospheres) using different methods (hot-injection, solvothermal/hydrothermal process, spray deposition, electrospun, and precursor process), which effected the catalytic performance for reduction of I_3^- (Krishnaiah *et al*., 2016).

Shuang *et al.* (2018) directly synthesised CZTS nanoplates on a FTO substrate as an efficient CE for DSSCs, the PCE of it is comparable to that of platinum (Pt) based counter electrodes in DSSC. Zhengfu *et al.* (2014) prepared the CZTS with various $\frac{[Cu]}{[Sn]+[Zn]}$ molar ratios, which show superior catalytic activity for I_3.

Chen *et al.* (2012) focuses on the improvement of crystallization of CZTS film for better catalytic activity for I_3 in DSSCs. Krishnaiah *et al*. (2016) reported CZTS nanocrystals (NCs) followed by selenisation and obtained CZTSSe, then employed it as CE for DSSC, the PCE significantly increased. The above studies have made achievements in the improved performance *via* employing CZTS or CZTSSe as CE for DSSCs. Although CZTS(Se) showed excellent catalytic ability for I_3, the exact reason for good electro-catalytic activity of CZTS(Se) is not clear, and the role of each atom of the material has also not been clarified. It must be greatly meaningful to explore catalytic mechanism of each active site in an effective way.

The first-principles calculations based on the density functional theory (DFT) is an extremely effective method to investigate the catalytic mechanism at the I_3 molecules/catalyst interface by the adsorption energy, density of states (DOSs), and electron density difference (EDD). Shuang *et al.* (2018) reported that CZTS was synthesised and used as CE material for DSSCs. The PCE of DSSC that resulted was 7.13 % which can be comparable to that of Pt-based DSSCs (7.62 %).

Hydrothermal method is a non-vacuum method of nano-particle synthesis that does not require any expensive precursors or equipment and can be readily adopted for industrial production processes. It possesses remarkable reliability and selectivity as well as high efficiency at low temperature. Hydrothermal method have been developed to prepare CZTS nanoparticles. The hydrothermal method is defined as a method that uses water as a solvent in a sealed reaction container when the temperature is raised above 100 °C (Habib, 2012).

Hydrothermal synthesis is usually undertaken in an autoclave, normally consisting of a stainless steel shell with a Teflon liner. The function of an autoclave is to withstand the internal pressures developed during the hydrothermal process, while the inert liner is used to protect the stainless steel outer shell from the corrosive reagents used in material synthesis (Habib, 2012).

Polymer based surfactants have been reported to have been widely used in hydrothermal method of preparing inorganic nanomaterial oxides and sulphides. Such surfactants reported are polyethylene glycol (PEG), polyacrylic acid (PAA), polyvinyl alcohol (PVA) and polyvinylpyrrolidone (PVP). These polymers acts as structure directing agents which can control the morphology and size of particles formed in hydrothermal process (Tiong *et. al*., 2014)

Hydrothermal synthesis of CZTS nanocrystals was firstly reported by Wang *et al*. (2011) by dissolving copper (I) chloride (CuCl), zinc chloride ($ZnCl_2$), tin (IV) chloride pentahydrate ($SnCl_4 \cdot 5H_2O$) and thiourea in water followed by hydrothermal treatment at 200 °C for 30 h.

Agglomerate plate-like nanocrystals with average diameters ranging from 5 - 7 nm were observed. The band gap of the material was found to be 1.7 eV. Binary products such as ZnS and SnS_2 were found in the hydrothermal product when the reaction temperature and duration were reduced. They concluded that a reaction temperature above 200 °C was necessary to produce CZTS without impurities. However, Verma *et al.* (2013) used lower reaction temperature (180 °C) and duration (16 h) in a hydrothermal synthesis to produce pure phase CZTS material. They have also suggested that the hydrothermal method is a better route to yield pure phase CZTS compared to the solvothermal synthesis approach which uses ethylenediamine (EN) as solvent in the precursor solution. Metal ions are suspected to have complex with thiourea to form metal-thiourea complexes prior to hydrothermal reaction. During the hydrothermal treatment, hydrogen sulphide (H_2S) is produced through decomposition of thiourea, which then acts as the sulphur source for the formation of binary sulphide products. The reaction of the binary sulphides leads to the formation of CZTS.

With the introduction of ethylenediamine (EN) (volume ratio of EN : water = 1 : 9) in water, Liu *et al*. (2013) synthesised CZTS nanoparticles. In their experiment, hydrothermal treatment was carried out at 180 °C for 24 h and thiourea was used as the sulphur source. However, the XRD pattern shows impurities in the final product

which were not identified by the authors. Irregular sphere shape and nearly mono dispersed CZTS nanocrystals with sizes in the range of 5 ± 0.5 nm were resolved using TEM. In another report, band gap tuneable hydrotropic CZTS nanocrystals were produced by employing the same precursor solution and hydrothermal treatment. CZTS nanocrystal size was found to vary from 3 - 10.5 nm when the reaction duration was extended from 6 - 48 h. Peak broadening and blue shift (~2 cm^{-1}) in the Raman scattering spectrum of the CZTS nanocrystals were detected when the size of the nanocrystals decreased. These asymmetric broadening and shift of Raman bands are attributed to the broadening of the phonon momentum based on the Heisenberg uncertainty principle (Liu, *et. al*., 2013). A similar blue shift in the bandgap measurement of the CZTS nanocrystals (from 1.48 - 1.89 eV) was also observed with the reduction in nanocrystals size, which is caused by optical quantum confinement. EN was proposed to play an important role in increasing the hydrophilism. EN also acts as a capping ligand which binds to the nanocrystal surface to reduce the growth of CZTS crystals.

Unique CZTS microspheres (sizes: 4 - 8 μm) were synthesised through the utilization of hydrothermal conditions at 190 °C for 24 h in the presence of citric acid with metal chlorides and thiourea (Sarkar *et. al*., 2014). In this hydrothermal reaction, citric acid played an important role in reducing the segregation. In the meantime, citric acid also helped the formation of the microspheres structure of CZTS by controlling the crystal growth. A possible nucleation-dissolution-recrystallisation growth mechanism has been proposed based on the time-dependent investigation of the hydrothermal product. The photo-response of the as-deposited CZTS films was found to increase with the increase in citric acid concentration in the reaction system.

In a separate study, Jiang *et al*. (2015) reported a metastable orthorhombic phase of CZTS using thiocarbamide as the sulphur source and a solvent mixture of water and EN (volume ratio = 1 : 1).The hydrothermal reaction was performed at 200 °C for 24 h. The crystal phase was found to gradually transform from kesterite to orthorhombic structure with the increase of the concentration of EN. The orthorhombic CZTS transformed to kesterite CZTS through a heat treatment at 500 °C for 2 h. The electrical properties of the orthorhombic CZTS were evaluated and the CZTS film was discovered to perform as a photoresistor.

The inorganic sulphur source approach was introduced by Jiang & Yan (2015) who substituted the commonly used thiourea or thioacetamide with sodium sulphide nanohydrate ($Na_2S·9H_2O$) in the hydrothermal reaction. A CZTS material was obtained by hydrothermally treating the precursor solution containing the corresponding metal chlorides and Na_2S at 230 °C for 24 h. However, pure phase CZTS materials were not obtained. Impurities of Cu_2SnS_3 and $Cu_{2-x}S$ were found to coexist in the final synthesised product. Two reaction routes were proposed in this system: (i) Direct formation of ternary and binary products, Cu_2SnS_3 and ZnS, respectively, leading to the formation of CZTS; (ii) Formation of CZTS through binary products, Cu_2S, SnS_2 and ZnS. Although the size distribution of the resulting CZTS products and the homogeneity of the deposited film in terms of surface coverage were poor, the heat treated CZTS film (at 450 °C for 1 h under N_2 flow) exhibited remarkable photocurrent and voltage under light illumination in a photoelectrochemical measurement.

Chopra *et al*. (2024) synthesized nanocrystalline CZTS powder through hydrothermal process, using thiourea as sulphur precursor. They got kesterite CZTS of particle size 4-5nm.High-temperature thermal annealing treatments are needed for the as-deposited nanocrystal films to form large grains, which are crucial for high performance thin film solar cells. Based on the experience with CIGS and CIS film deposition for solar cells, films with micrometer sized grains in the absorber layer can produce cells with high power conversion efficiencies. The current progresses in CZTS nanocrystal based solar cells have demonstrated that without a grain-growing thermal treatment process, solar cells are generally unable to generate 1% efficiency.

Weber *et. al.* (2010) reported that even when kesterite crystal structure nanocrystals have been formed in deposited films, thermal annealing cannot be omitted. To make CZTS thin films from the nanocrystals, CZTS nanocrystals are generally dispersed in a solvent or a mixture of solvent and binder before being subjected to film deposition. The CZTS slurry or paste with suitable rheological properties must be prepared to create a uniform layer with homogenous film thickness. The nanocrystal coatings are normally accomplished by either repeating spin coating or doctor-blading to achieve 1 to 2 μm of film thickness, which is mostly reported as the absorber layer thickness for thin film solar cells. The as-deposited film is usually subjected to soft baking at a temperature around 300 °C, followed by a high temperature annealing at 500 to 580 °C for a designed duration. Although CZTS nanocrystals already contain the necessary amount of chalcogen (sulphur in most cases), the thermal annealing process of the nanocrystal films still requires the presence of chalcogen vapour. Under high vacuum conditions, the CZTS phase decomposes at temperature above 550 °C due to the volatilisation of SnS and elemental sulphur (Weber *et al*., 2010). The decomposition rate largely varies depending on the temperature, total pressure of the annealing chamber, and the partial pressure of the volatile products. Therefore, in order to prevent the loss of CZTS phase and the formation of undesired phases, an atmospheric base pressure and a chalcogen source are normally applied in the thermal annealing process. Continuous supply of

sulphur (sulphurisation) or selenium (selenisation) is a reasonable option to prevent the decomposition of CZTS and CZTSe.

Zhou *et al*. (2010) reported a simple and low cost screen printing approach for the preparation of CZTS thin film. Microparticles of CZTS prepared using wet ball milling and sintering methods, were dispersed in isopropanol. Separately, ethyl cellulose was dissolved in isopropanol. The screen printable paste was then made by mixing both solutions with small quantity of terpinol and deposited onto 'Mo' coated polyimide substrates. Band gap, sheet resistance, carrier concentration, and Hall mobility of the screen printed CZTS layers were 1.49 eV, 2.42×10^3 Ω/cm, 3.81×10^{18} cm^{-3}, and 12.61 $cm^2V^{-1}s^{-1}$ respectively. The aim of this research work is to optimise the use of polyacrylic acid as surfactant in hydrothermally synthesised Cu_2ZnSnS_4 thin films for application as counter electrode in dye sensitised solar cell.

MATERIALS AND METHODS

0.2 mmol of $CuCl_2.2H_2O$, 0.1 mmol of $ZnCl_2$, 0.1 mmol of $SnCl_4.5H_2O$, 0.5 mmol of C_2H_5NS and the quantity of PAA surfactant was varied as 0.0 g, 0.6 g, 1.0 g and 1.4 g, were in each case dissolved in 36 ml of water under magnetic stirring. The resulting solution was transferred to a Teflon-lined stainless steel autoclave of 45 ml capacity, which was then sealed and in each case maintained at 150 ºC for 24 h, and the autoclave in each case was allowed to cool to room temperature naturally. The black precipitate that resulted from the autoclaving of each sample was centrifuged and washed with deionised water, absolute ethanol and acetone for several times. Finally, the products were vacuum-dried at 80 °C for 5 h. The dried powders obtained from as-synthesised CZTS nanocrystals were prepared for thin film deposition by dispersing the CZTS powder (10%, w/w) in mixture of terpineol and triton X-100 (85%:5%, w/w). The slurry was then subjected to rigorous magnetic stirring at 450 RPM for 48 h.

Thin films were then prepared by depositing the CZTS slurry on FTO coated soda lime glass (FTO/SLG) substrate by doctor-blading. Before deposition on the substrate, it was prewashed thoroughly with deionised water, acetone, and ethanol in sequence under sonication for 10 min each followed by being blow-dried with nitrogen gas. The thin films after deposition were then placed in a graphite box containing sulphur powder and annealed at 550 °C for 30 min in a rapid thermal annealing processing (RTP) system with a heating rate of 10 °C/min. A static annealing atmosphere of 0.3 atm argon was supplied in the RTP furnace.

The TiO_2 thin films to be used as photoanodes were synthesised on well cleaned FTO glass by doctor blading method. A transparent layer of TiO_2 thin film was prepared by weighing its nano particles powder and dissolving in deionised water (0.5 M) and then it was coated on the FTO glass. The as-deposited TiO_2 layers were gradually heated to 500 ºC to bake and kept at that temperature for 3 hours. The films after baking were further treated in 0.05M $TiCl_4$ solution for 1 h, then rinsed, dried and heated to 500 ºC for 0.5 h again. After the temperature has cooled down to 80 ºC, they were immersed into an ethanol solution of 0.5 M N719 dye ($RuL_2(SCN)_2.2H_2O$, L = 2,2-bipyridyl-4,4-dicarboxylic acid, Dyesol, 0.3 mM) for 24 hours. The dye sensitised TiO_2 films were then rinsed with ethanol and dried in air to be used as the photoanode in the dye sensitised solar cell.

The sandwich type solar cell comprised of a sensitised TiO_2 photoanode as the working photoelectrode, as-prepared CZTS/FTO thin films as the CE, and a redox mediator solution containing 0.1 M LiI, 0.05 M I_2, 0.6 M 1,2-dimethyl-3-n-propylimidazolium iodide and 0.5 M 4-tert-butylpyridine in acetonitrile as electrolyte. The two electrodes (photoanode and counter electrode) were clamped together using binder clips and in-between the two electrodes, silicon gum was used to seal the edges and electrolyte was injected in between the electrodes. The effective area of the resulting cell was 1.0 cm x 0.5 cm after the assembly of the DSSC was completed.

Characterisation

The crystallographic structure and phase analysis of the synthesised thin film samples were done by X-ray diffraction (XRD, PANanalytical XPert Pro Multi-Purpose Diffractometer (MPD), CuKα, λ = 0.154056 nm). The Raman spectra of the samples were recorded with a Raman spectrometer (Xplora Plus, Horiba Scientific Raman microscope) with a 785 nm excitation laser to distinguish possible secondary phases in the films.

The morphology and quantitative elemental analysis of the samples were characterised by scanning electron microscopy (SEM, JEOL 7600F) at an acceleration voltage of 20.0 kV combined with an energy dispersive X-ray spectroscopy (EDS). Surface roughness and topology measured using (Hitachi 5100N) atomic force microscope (AFM).

Ultraviolet-visible (UV-vis) absorption spectrum of the samples was measured at room temperature using a Shimadzu UV-1800 spectrophotometer. The reflected light was not considered in the UV-Visible light absorption measurement. The Infra-red spectra of the samples were measured using Perkin-Elmer, G-FTIR spectrometer.

The thickness of the films was measured using Alpha step Q 7083319 surface profiler, while the electrical resistivity measurement of the thin film samples was done using (signatone PRO 4, LUCAS LABS 2400) four point probe. The assembled DSSC was characterised using the solar simulator to determine the I-V characteristics with an AM 1.5 solar simulator equipped with a 450 W xenon lamp (Model No. 81172, Oriel).

RESULTS AND DISCUSSION

The XRD pattern of the CZTS thin film samples are shown in the Figure below.

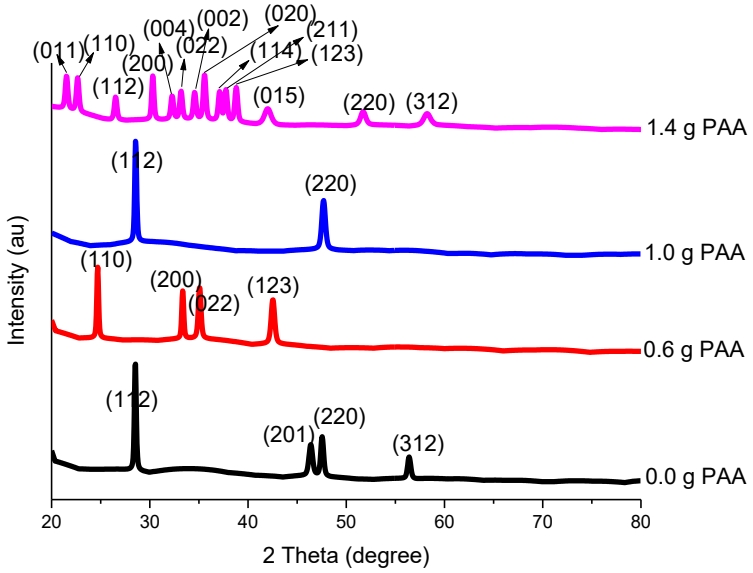

Figure 2: XRD patterns for CZTS thin film samples

Variations in the PAA amount play a vital role in the structure formation of the thin film material. Two of the films show preferential orientation along (112) plane (that the one synthesised using 1.0 g and 0.0 g). From the XRD peaks, the 2Θ values chosen for calculation were 28.59° corresponding for sample 1.0g and 28.64 also corresponding to (112) plane for 0.0 g. The XRD pattern also confirms the formation of CZTS in all the films but a high amount of impurity was observed in sample 1.4 g PAA which is evident with the numerous peaks observed in the spectra. Samples 0.0 g PAA and 0.6 g PAA also shows the presence of secondary phases. With the increase of PAA content in the precursor solution, improved crystallinity of the synthesised product was observed from 0.0 g up to 1.0 g. The results suggest that the presence of PAA in the precursor solution not only significantly influence the crstallinity of the particles, more importantly, PAA determines the formation and purity of the synthesised CZTS product. Crystallite size of the films also varies with variation in PAA amount.

Table 1: FWHM and Crystallite size of CZTS thin film samples

Sample Name	2Θ (°)	FWHM (°)	d-spacing (Å)	h k l	Average Crystallite Size (nm)	Lattice Parameters	
						a (Å)	c (Å)
1.4gPAA	21.50	14.24	4.13277	011	15	5.43	010.86
	22.63	29.52	3.92776	110	19		
	26.49	29.52	3.36435	112	17		
	30.28	24.60	2.95163	013	19		
	32.24	29.52	2.77613	004	11		
	33.16	29.52	2.70149	022	13		
	34.53	29.52	2.59705	002	11		
	36.54	29.52	2.52548	020	17		
	37.07	29.52	2.42473	114	15		
	37.77	29.52	2.38469	211	09		
	38.76	29.52	2.32281	123	07		
	41.97	78.72	2.15270	015	11		
	51.67	59.04	1.76905	031	13		
	58.18	78.72	1.58564	224	17		

1.0gPAA	28.59	14.30	3.12209	112	19	5.43	010.86
	47.70	34.95	1.90657	024	14		
0.6gPAA	24.67	14.26	3.60844	110	18	5.43	010.86
	33.33	19.68	2.68831	004	19		
	35.05	29.52	2.56047	022	11		
	42.49	39.36	2.12736	123	17		
0.0gPAA	28.64	10.22	3.11739	112	10	5.43	010.86
	46.01	98.40	2.92608	220	19		
	47.71	68.88	1.90616	024	15		
	58.25	28.13	1.33013	224	11		

The Raman spectra show the peaks 338 cm^{-1}, 257 cm^{-1}, 287 cm^{-1}, 368 cm^{-1} and 351 cm^{-1} which are CZTS peaks (Ahn *et. al*., 2010; Fernandes *et al*., 2009). For 1.4 g PAA, peaks 275 and 315 appeared which are for ZnS and SnS_2 secondary phases respectively (Nagoya *et al*., 2010; Price *et al*., 1999). The 476 cm^{-1} $Cu_{2-x}S$ secondary phase peak also appeared in sample 0.0 g PAA (Fernandes *et al*., 2009). It can be inferred that only at 1.0 g PAA that gave pure phase CZTS compound. At lower PAA amounts, presence of secondary phases was observed. Also at higher amount, secondary phases were seen.

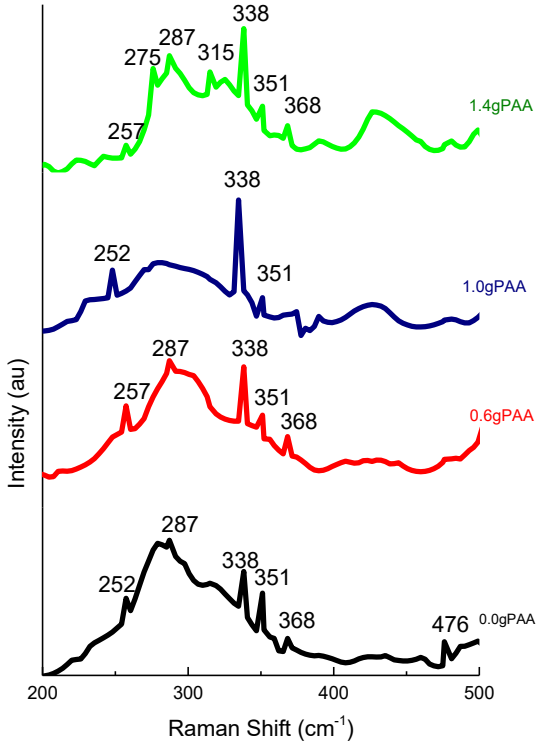

Figure 3: Raman spectra for CZTS thin films

The SEM images demonstrate the morphology evolution of the samples with the increase of PAA amount in the precursor solution. Few spherical shaped particles were obtained when there was no PAA in the precursor solution. With 0.6 g of PAA added to the solution, flower-like particles which are composed of several spheres were formed. When the amount of PAA was increased to 1.0 g and 1.4 g, sphere-like agglomerates of particles were formed

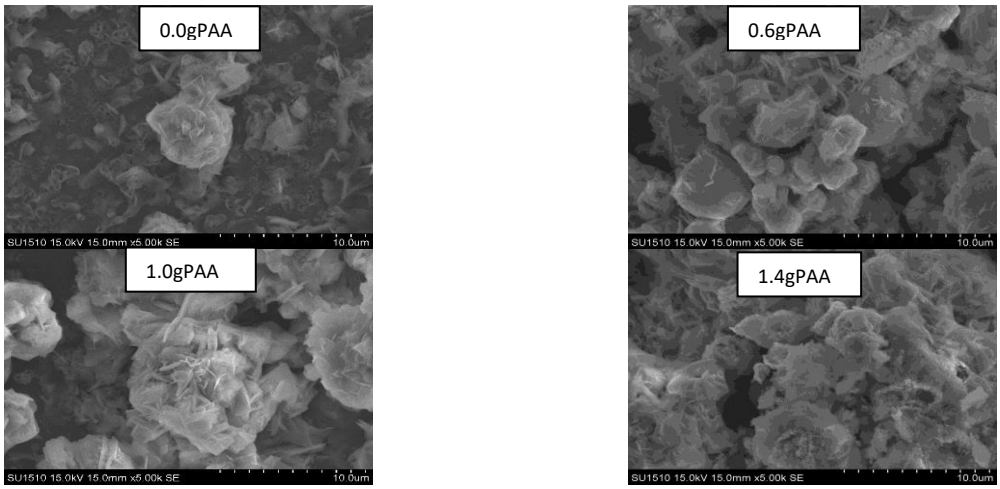

Figure 4: SEM images for CZTS thin film samples

The atomic percentage of Cu and S did not show significant changes as for sample synthesized using 0.6 g PAA and 1.4 g PAA surfactants. The 0.6 g PAA and 1.0 g PAA samples reveal near ideal compositional ratio for Cu/Zn + Sn of 0.81 and 0.91, Zn/Sn ratio of 0.75 and 0.87 respectively, these values though shows they are both Cu poor and Zn poor. Cu/(Zn + Sn) atomic ratio of near 0.85 have however been reported to show good optoelectronic properties and best device efficiency. The slightly Sn rich and Zn poor composition for 0.6 g PAA and 1.0 g PAA may be ascribed to the reactivities of the different metal precursor. The Cu:Zn:Sn:S ratios of 1.87:1.00:1.34:4.09 and 1.97:1.00:1.35:4.17 for the 0.6 g PAA and 1.0 g PAA samples respectively were close to ideal stoichiometric value of 2:1:1:4. Samples 0.0 g PAA and 1.4 g PAA however show significant deviation from ideal CZTS composition exhibiting very high Cu and S content. These samples show significant decrease in the Zn/Sn ratio. The Zn/Sn ratios shows the samples are Sn rich and Zn poor, with 0.0 g PAA and 1.4 g PAA showing significantly high Sn content compared to Zn.

Table 2: EDS Data for CZTS Thin Film

Sample ID	Cu (at.%)	Zn (at.%)	Sn (at.%)	S (at.%)	$\frac{Cu}{Zn+Sn}$	$\frac{Zn}{Sn}$	Cu/Zn/Sn/S
0.0 g PAA	22.9	7.3	17.7	48.6	0.92	0.41	3.14:1.00:2.42:6.66
0.6 g PAA	22.0	11.6	15.5	47.4	0.81	0.75	1.87:1.00:1.34:4.09
1.0 g PAA	23.1	11.8	13.5	48.9	0.91	0.87	1.97:1.00:1.35:4.17
1.4 g PAA	22.3	7.6	19.7	48.0	0.82	0.39	2.93:1.00:2.59:6.32

The AFM 3D surface visualization of the CZTS thin film shows granular variations. The values of roughness shows that samples 1.4 g PAA (1.5 x 10^3 nm), 1.0 g PAA (0.8 x 10^3 nm), 0.6 g PAA (1.0 x 10^3 nm) and 0.0 g PAA (1.5 x 10^3 nm). These values show that the surfaces are quite smooth to allow good physical contact with the subsequent layer and can avoid the shorting that may arise due to contacts with the electrolytes in DSSC's.

Figure 5: AFM images for CZTS thin film samples

The direct band gap Eg was calculated by extrapolating the linear portion of the curves of $(\alpha h\nu)^2$ vs. $(h\nu)$ to give the values of Eg as follows; 1.63 eV for sample 1.4 g PAA, 1.51 eV for sample 1.0 g PAA, 1.70 eV for sample 0.6 g PAA and 1.52 eV for sample 0.0 g PAA (Figure 4.20 below) . These band gap values are in good agreement with the reported value in literature (Chalapathiu *et al*., 2015).

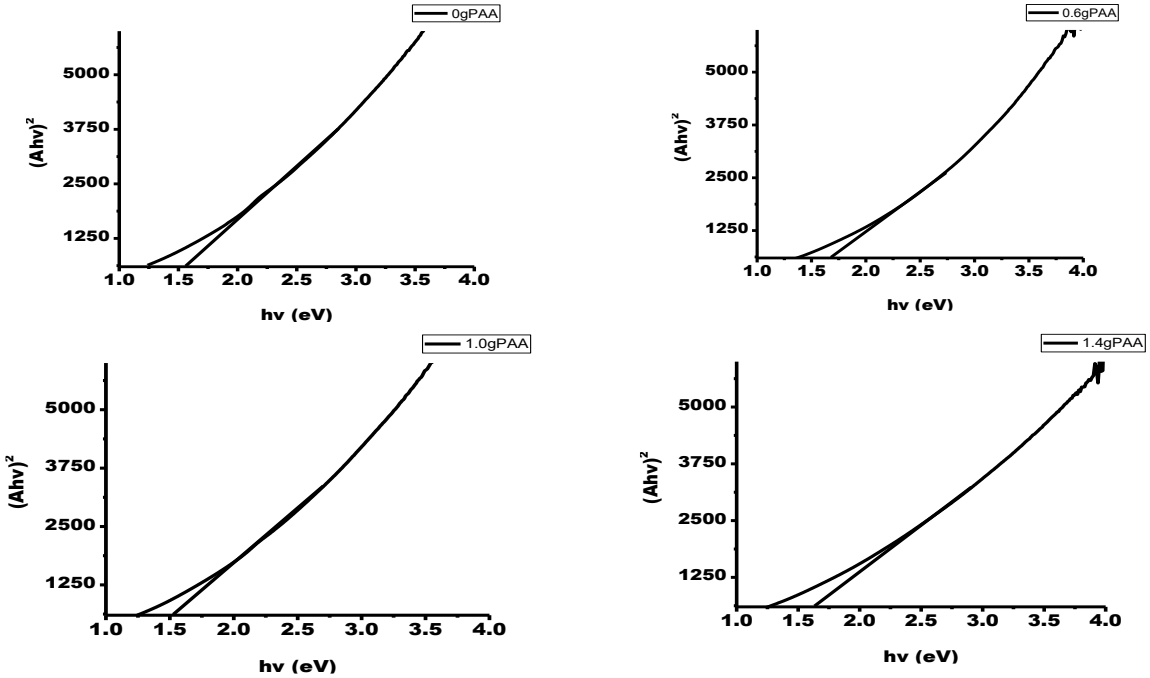

Figure 6: Energy band gap spectral analyses for CZTS thin film samples

All the resistivity values obtained exhibited the p-type material property of 10^{-2} Ωm as shown in Table 3 below. The resistivity values for 0.0 g PAA and 1.0 g PAA recorded higher values as compared to 1.4 g PAA and 0.6 g PAA samples. The high value resistivity for 0.0 g PAA could be due to the fact that there was no surfactants to control the growth of crystals in the CZTS material thus for very small crystals. The impurities in the material can increase its resistivity.

Table 3: Resistivity of CZTS thin film samples

Sample Name	Resistivity (Ωcm)
1.4 g PAA	1.71×10^{-2}
1.0 g PAA	4.03×10^{-2}
0.6 g PAA	1.86×10^{-2}
0.0 g PAA	5.14×10^{-2}

Results from the photovoltaic Characterisation of the dye sensitised solar cell, all the samples have same open circuit voltages of 0.475 V. Considering the short circuit currents, the sample 0.0 g PAA has a lower value of 1.900 mA/cm^2 when compared the other samples which could be attributted to the presence of high level of secondary and ternary phases in the counter electode as revealed in the XRD and Raman spectra. This can be attributed to the

weak chellation of the sample as no surfactant was present (Walsh *et al*., 2012). The samples 1.4 g PAA and 0.6 g PAA have higher short circuit currents of 3.800 mA/cm^2 while sample 1.0 g PAA had the highest value of 9.500 mA/cm^2 which is the sample with pure CZTS phase. The presence of secondary and ternary phases in counter electrode CZTS material tends to create shunting paths which adversely affect the rgeneration of I^- from I^{3-} (Wu *et al*., 2007). The efficiency of the DSSC solar cell with the highest value was the sample 1.0 g PAA (3.200%) this value is comparable to Chen et al. (2015) that used CZTS counter electrode prepared solvothermally and deposited using drop casting with 3.22 % energy conversion efficiency of the cell. Abermann (2013) also obtained 3.10 % energy conversion efficiency using CZTS film synthesis using hydrothermal and spin coating the film on FTO glass used as counter electrode. The next higher value is 1.490% for the materials with the next better quality(1.4 g PAA and 0.6 g PAA). While for the sample synthesised using 0.0 g PAA surfactant yielded 0.902% energy conversion efficiency. It is clear from the results that counter electrode quality plays a vital role in determining the energy conversion efficiency of the dye sensitised solar cell. It is also clear that the values obtained were lower than some of the values reported in the literature (Shuang *et al*., 2018). These low values could be attributtable to the absorption electrode and also the electrolyte since they were not optimised.

CONCLUSION

The work demonstrated that the synthesis of CZTS compounds with different crystal structure and size could be achieved using a water-based hydrothermal system. The precursor materials especially the polymer surfactants were able to reveal its ability for the control and determine the different crystals structure of CZTS, surfactants were found to play the roles of determining the purity and phases of CZTS compound, as well as controlling the crystal growth of CZTS nanocrystals. The slurry that was developed in this work was used in depositing uniform and compact nanoparticle-based films. Finally, the best CZTS thin film materials in terms of desirable properties were used for dye sensitised solar cell counter electrode. The optimised CZTS material when used as counter electrode in dye sensitised solar cell yielded the highest energy conversion efficiency of 3.200 %. The findings in this project may inspire scientists to discover novel materials with interesting properties and may act as a stepping stone towards the fabrication of high efficiency solar cells. The study on the optimisation of dye sensitised solar cell fabrication and factors affecting the cell's performance was not carried out in this research. Therefore, future work should focus on the optimisation solar cell fabrication and identify the limiting factors towards high performance solar cell devices. The electrical properties of devices should also be assessed to optimise the power conversion efficiency (PCE) of the devices. The limitations in supply of platinum, open circuit voltage (*Voc*) and short circuit current (I_{SC}) are some of the most important issues that dye sensitised solar cell devices are currently facing. One of the possible ways to solve this is by replacing the most commonly used platinum counter electrode with CZTS and optimise all the components (Photoanode, Electrolyte and counter electrode) of the cell.

REFERENCES

Ahn, D., Brag, H. O. & Zhika, D. (2010). *The physics of solar cells*. Imperial college press, London. 29-37.

Anurag, R., Parukuttaymma, S. D., Smagul, K., Mamedov, D., Tapas, K. M. & Senthilarasu S. (2018). A review on applications of Cu_2ZnSnS_4 as alternative counter electrodes in dye sensitized solar cells. *AIP advances*, (8), 701-707.

Chalapathi, U., Uthanna, S. & Raja, S. (2015). Growth of Cu_2ZnSnS_4 thin films by a two stage process-Effect of incorporating of sulfur at the precursor stage. *Solar Energy Materials and Solar Cells,* (132), 476-484.

Chang, S. H., Lu, M. D., Tung, Y. L. & Tuan, H. Y. (2013). Gram-scale synthesis of catalytic Co_9S_8 nanocrystal ink as a cathode material for spray-deposited, large-area dye-sensitized solar cells. *ACS Nano,* (*7*), 9443-9451.

Chopra, K. L., Paulson, P. D. & Dutta, V. (2024). Thin film solar cell: an overview. *Programmed Photovolt: Research Application*, (12), 69-92.

Fernandes, M., Cao, L., Zhang, B. L. & Jiang, J. C. (2009). One step deposition of CZTS thin films for solar cells. *Solar Energy Materials and Solar Cells*, (117), 81-86.

Habib, S. L., Idris, N. A., Ladan, M. J. & Mohammed, A. G. (2012).Unlocking Nigeria's solar PV and CSP potentials for sustainable electricity development. *International Journal of Scientific and Engineering Research,* (5), 2010-2012.

Hardin, B. E., Snaith, H. J. & McGehee, M. D. (2012). The renaissance of dye sensitised solar cells. *Nature photonics*, (6), 162-169.

Ito, K. & Nakazawa, T. (1988). Electrical and optical properties of stannite-type quaternary semiconductor thin films. *Japanese Journal of Applied Physics,* (11), 2094-2097.

Jiang, M. & Yan, X. (2015). Cu_2ZnSnS_4thin film solar cells: Present status and future prospects. *Solar Cells – Research and Application Perspectives,* (108), 107-117.

Jiang, C. S., Repins, I. C., Montinho, H. R., Ramanathan, K. & Aljassinn M. M. (2015). Investigation of micro-electric properties of CZTS thin films using scanning probe microscopy. *Solar Energy Materials and Solar Cells,* (132), 342-347

Krishnaiah, M., Anvita, K., Chaitanya, B., Parag, B. & Sudhanshu, M. (2016). Effect of solvent reaction time on morphology of Cu2ZnSnS4 (CZTS) nanoparticles and its application in dye sensitized solar cells. *Materials today: proceeding*, (3), 1778-1784.

Liu, W., Guo, B., Mak, C., Li, A., Wu, X. & Zhang, F. (2013). Facile synthesis ultrafine Cu_2ZnSnS_4 nanocrystals by hydrothermal method for use in solar cells. *Thin solid films*, (535), 39-43.

Malerba, C. (2014). An investigation into the stoichiometry effect on CZTS microstructure and optoelectronic properties. *Solar Energy Materials and Solar Cells,* (97), 433-438.

Nagoya, K. V., Pawara, S. M., Shinb, S. W., Moona, J. H. & Kima, P. S. (2010). Electrosynthesis of CZTS films by sulfurization of CZT precursor: effect of soft annealing treatment. *Applied Surface Science*, (238), 74-80.

Price, D. B., Mitzi, O., Gunawan, T. k. & Wang, K. (1999). The path towards a high performance solution-processed kesterite CZTS. *Solar Energy Materials and Solar Cells,* (95), 1421-1436.

Sarkar, S., Bhattacharjee, K., Das, G. C. & Chattopadhyay K. K. (2014). *CrystEngComm. Royal Society of Chemistry*, (16), 2634-2644.

Shuang, L., Huanying, Y., Fei, L., Yinglin, W., Shixin, C., Guochun, Y., Yichun, L. & Xintong, Z. (2018). Element substitution of kesterite Cu_2ZnSnS_4 for efficient counter electrode of dye sensitized solar cells. *Scientific reports*, (8), 8714-8717.

Tiong, T. T., Hreid, T., Will, G., Bell, J., & Wang, H. (2014). Polyacrylic acid assisted synthesis of CU_2ZnSnS_4 by hydrothermal method. *Science of Advanced Materials*, (6), 1467-1474.

Verma, S. K., Agrewal, V., Jain, K., Pasricha R. & Chand S. (2013). Green synthesis of nanocrystalline Cu_2ZnSnS_4 powder using hydrothermal rout. *Journal of nanoparticles*, (203), 1-7.

Wadia, C., Alivisatos, A. P. & Kammen, D. (2009). CZTS-based solar cell from sol-gel spin coating and its characterization. *Evironment Science and Technology,* (43), 2072-2077.

Wang, K., Mitzi, D. B., Barkhouse, R. & Aaron, D. (2011). Prospects and performance limitations for Cu-Zn-Sn-S-Se photovoltaic technology. *Philadelvia Transnational Royal Society,* (371), 1-22.

Washio, T., Shinj, T., Tajima, S., Fukano, T., Motohiro, T., Jumbo, K. & Katagari, H. (2015). Study of optical and structural properties of CZTS thins films grown by co-evapouration and spray pyrolysis. *Iopscience,* (65), 141-145.

Weber, R., Ishino, K., Moritake, R. & Minemoto, T. (2010). Improvement of CZTS thin film morphology using Cu-Zn-Sn-O precursor grown from sputtering. *Current Applied Physics*, (13), 1861-1870.

Wei, W., Sun, K. & Hu, Y. H. (2016). An efficient counter electrode material fordye-sensitized solar cells-flower-structured 1T metallic phase MoS_2. *Journal of Materials Chemistry*, (4), 12398-12401.

Yan, H., Jiao, Y., Wu, A., Tian, C., Zhang, X., Wang, L., Ren, Z. & Fu, H. (2016). Cluster- like molybdenum phosphide anchored on reduced graphene oxide for efficient hydrogen evolution over a broad pH Range. *Chemistry Communication*, (52), 9530-9533.

Yang, W., Xu, X., Li, Z., Yang, F., Zhang, L., Li, Y., Wang, A. & Chen, S. (2016). Construction of efficient counter electrodes for dye-sensitized solar cells: Fe_2O_3 nanoparticles anchored onto graphene frameworks. *Carbon*, (96), 947-954.

Zhou, Z., Wang, Y., Xu, D.& Zhang, Y. (2010). Fabrication of Cu_2ZnSnS_4 screen printed layers for solar cells. *Solar Energy Materials and Solar Cells*, (94), 2025-2042.